Volumetric intensity dependence on the formation of molecular and atomic ions within a high intensity laser focus

ARTICLE *in* JOURNAL OF THE AMERICAN SOCIETY FOR MASS SPECTROMETRY · FEBRUARY 2005

Impact Factor: 2.95 · DOI: 10.1016/j.jasms.2004.09.018 · Source: PubMed

11 AUTHORS, INCLUDING:

Paul Mckenna
University of Strathclyde
218 PUBLICATIONS **2,914** CITATIONS
SEE PROFILE

Thomas Mccanny
University of Strathclyde
89 PUBLICATIONS **2,052** CITATIONS
SEE PROFILE

Jiamin Yang
Research Center of Laser Fusion, P.R.China
112 PUBLICATIONS **651** CITATIONS
SEE PROFILE

Johan Mauritsson
Lund University
92 PUBLICATIONS **1,926** CITATIONS
SEE PROFILE

Volumetric Intensity Dependence on the Formation of Molecular and Atomic Ions within a High Intensity Laser Focus

Lynne Robson, Kenneth W. D. Ledingham,* Paul McKenna, Thomas McCanny, Seiji Shimizu,† and Jiamin M. Yang‡
Department of Physics, University of Strathclyde, Glasgow, Scotland, United Kingdom

Claes-Göran Wahlström, Rodrigo Lopez-Martens, Katalin Varju, Per Johnsson, and Johan Mauritsson
Department of Physics, Lund Institute of Technology, Lund, Sweden

The mechanism of atomic and molecular ionization in intense, ultra-short laser fields is a subject which continues to receive considerable attention. An inherent difficulty with techniques involving the tight focus of a laser beam is the continuous distribution of intensities contained within the focus, which can vary over several orders of magnitude. The present study adopts time of flight mass spectrometry coupled with a high intensity (8×10^{15} Wcm^{-2}), ultra-short (20 fs) pulse laser in order to investigate the ionization and dissociation of the aromatic molecule benzene-d1 (C_6H_5D) as a function of intensity within a focused laser beam, by scanning the laser focus in the direction of propagation, while detecting ions produced only in a "thin" slice (400 and 800 μm) of the focus. The resultant TOF mass spectra varies significantly, highlighting the dependence on the range of specific intensities accessed and their volumetric weightings on the ionization/dissociation pathways accessed. (J Am Soc Mass Spectrom 2005, 16, 82–89) © 2004 American Society for Mass Spectrometry

The dynamics of atomic and molecular ionization in intense, ultra-short laser fields is a subject which continues to receive considerable attention among physicists and chemists. An inherent difficulty with techniques involving the tight focus of a laser beam is the continuous distribution of intensities contained within the focus. A consequence of such spatial focusing is that any gas-phase targets involved in a laser-molecule interaction are subject to both spatial and temporal variations in laser intensity [1, 2]. For a focused laser beam which is Gaussian in r (r $\perp$ to laser beam direction) and Lorentzian in z (beam direction) the intensity $I_{(r,z)}$ is given by [3],

$$I_{(r,z)} = \left[\frac{I_0}{1 + (z/z_0)^2}\right] \exp\left\{\frac{-2r^2}{W_0^2[1 + (z/z_0)]^2}\right\} \quad (1)$$

where I_0 is the peak intensity, w_0 is the minimum waist radius (at $1/e^2$ intensity) and z_0 is the Rayleigh range given by $\pi {w_0}^2/\lambda$ which corresponds to the distance along the beam axis (r = 0) where the intensity has fallen to half the maximum intensity. Rearranging equation 1 for r at $I = I_s$ where I_s is the saturation intensity (intensity at which the ionization probability approaches unity, leading to the depletion of atoms in the ionization volume) yields,

$$r = \frac{w_0^2}{2}[1 + (z/z_0)^2]\left[\ln\left(\frac{I_0/I_s}{1 + (z/z_0)^2}\right)\right]^{\frac{1}{2}} \quad (2)$$

which describes a contour surface shell of constant intensity I_s. These contours take the distinctive form of "peanut-shaped" lobes as depicted in Figure 1. For the focal parameters achieved in the present experiment at a peak intensity $I_o \sim 8 \times 10^{15}$ Wcm^{-2} it can clearly be seen that the largest fraction of the total Gaussian focal volume is occupied by lower intensities.

The majority of studies carried out using high intensity lasers coupled to time of flight (TOF) mass spectrometers has involved intensity averaged data collection, and the data is then interpreted by assuming that the ionization dissociation dynamics is governed by the peak laser intensity at the center of the focus. This is a reasonable assumption considering the highly non-

Published online December 15, 2004

Address reprint requests to Dr. L. Robson, Department of Physics, University of Strathclyde, John Anderson Bldg., 107 Rottenrow, Glasgow G4 0NG, Scotland, UK. E-mail: l.robson@phys.strath.ac.uk

* Also at AWE plc, Aldermaston, Reading, UK.

† Present address: Institute for Chemical Research, Kyoto University, Gokasho, Uji, Kyoto 611-0011, Japan.

‡ Present address: Research Center of Laser Fusion, P.O. Box 919-986, Mianyang 621900, People's Republic of China.

1044-0305/05/$30.00
doi:10.1016/j.jasms.2005.09.018

Received August 4, 2004
Revised September 21, 2004
Accepted September 21, 2004

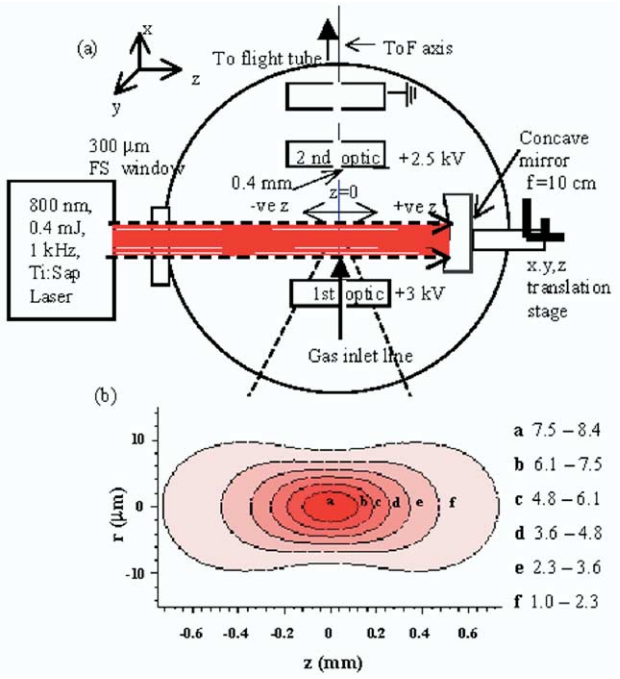

Figure 1. (**a**) Experimental set up for z-scan measurements. (**b**) Intensity distribution I (r,z) within the focal volume generated in the present experiment for a peak intensity of $I_o \sim 8 \times 10^{15}$ Wcm^{-2} depicted as isointensity contours. If rotated about the r = 0 axis, the distribution takes the form of 3-D "peanut-shaped" lobes. All intensities are given (x 10^{15} Wcm^{-2}).

linear behavior of intense field-induced ionization. However, several experiments have revealed important revelations concerning the shortcomings of intensity-averaged data collection. For example, studies have revealed that even in the case of atoms, subtle features of the ionization process may be masked by integration over the entire focal region [4, 5]. In a study by Hansch et al. [6], spatially dependent multiphoton multiple ionization of xenon was examined by scanning the focal volume across a pin hole (0.5 mm diameter) of the ionization region. Due to the spatial selectivity achieved using the 0.5 mm pin hole, the various charge states of Xe detected had very different volumetric weightings than those achieved in the conventional mode. El-Zein et al. [7] carried out a similar study for Xenon and characterized the laser confocal volume by cross-sections of the focus showing sequential ionization stages bounded by isointensity contours for Xe^+ to Xe^{6+}. The experimental ion yields were successfully explained by the theoretical expected volume behavior calculated using the appearance intensities of Augst et al. based on a barrier suppression scheme [8]. Additionally, Greenwood et al. applied the technique of "intensity selective scanning" to an Ar^+ ion beam target which revealed for the first time strong field ionization of high lying target metastable levels in an Ar^+ beam [9].

A recent study of intensity-selective field ionization of CS_2 by Banerjee et al. [1] used circular apertures of 2 and 15 mm placed at the entrance to the flight tube to spatially limit the interaction volume being sampled. The Rayleigh range was calculated as 2.4 mm. A strong molecular ion and dication were observed using the 15 mm aperture with S^{4+} the highest charged atomic ion observed at the peak intensity of 2×10^{15} Wcm^{-2}. In contrast, at almost the same absolute peak intensity, 3×10^{15} Wcm^{-2}, using the 2 mm aperture, a suppressed molecular ion was observed and no dication, but S^{5+} was present in the spectra recorded. It was concluded that in the former case, where the entire focal region was sampled, the low-intensity processes or "soft ionization" dominated the dissociation ionization dynamics. In contrast, when the 2 mm slit was introduced and aligned with the central point of the focal spot, only the highest intensity distribution was accessed, giving rise to a pronounced increase in multiply charged atomic ions. The work of Banerjee et al. has revealed important results concerning the spatial dependence of field induced dissociation of CS_2. It seems, however, that no experimental studies have been carried out to date concerning aromatic molecules or larger polyatomic molecules in relation to intensity selective scanning, where the effects of varying intensities within a laser focus could be even more significant due to competing ionization and dissociation processes. In the present work, the aromatic molecule benzene-d1 (C_6H_5D *m/z* = 79) is investigated in detail as a prototype aromatic. Benzene-d1 is chosen in favor of benzene to remove any ambiguity in discerning the doubly charged molecular ion, which for benzene-d1 lies at a half integer mass to charge ratio. Additionally, it has been known for some time that although the fragmentation and ionization for the same molecules presented by different groups using similar femtosecond lasers is qualitatively the same, quantitative differences exist [10]. Several possible explanations for this behavior exist, such as differing spatial and temporal pulse shapes, including different amounts of prepulse energy, as well as the magnitude of the ion extraction volume of the mass spectrometer. The following work addresses the sensitivity of relative ion yield and the yield of specific singly and multiply charged ions on the focusing geometry and alignment of the laser focus with respect to the TOF axis. Ultimately, the formation of singly and multiply charged molecular and atomic ions within a laser focus is probed.

Experimental

The reflectron time-of-flight (TOF) mass spectrometer used in this work has been described in detail elsewhere [11]. Briefly, the spectrometer comprises a stainless steel source chamber (see Figure 1) and a 1.5 m flight tube, both pumped by rotary-backed turbomolecular pumps to a base pressure of $\sim 2 \times 10^{-8}$ torr. Liquid-phase samples are contained in glass vials coupled to a bleeder valve on the spectrometer and the vapors are effusively admitted to the source chamber via a capillary tube. It is important to exclude any space-charge

effects [12], thus working pressures are kept to $\sim 10^{-7}$ torr to minimize such effects. Ion extraction and acceleration is achieved using an ion optic arrangement designed for this instrument (stainless steel discs, 50 mm diameter) based on Willey Mclaren principles [13]. Electrostatic potentials of +3 kV and +2.5 kV are applied to the first and second ion optic, respectively, to enable ion extraction, see Figure 1. The ions travel through the field-free flight tube into the two-stage reflectron [14] in order to correct any initial energy dispersion. The second ion optic (extraction optic) can be easily removed and replaced to allow extraction apertures of different sizes (0.8 mm wide slit or 0.4 mm diameter hole) to be inserted. The laser beam (λ = 800 nm, $\tau \sim$ 20 fs) is focused inside the chamber using a f =10 cm silver coated concave mirror. The minimum beam waist radius is estimated to be ~ 9 μm. This set up generates estimated intensities up to 8×10^{15} Wcm^{-2} which are also measured and verified [8] by the detection of Kr^{6+}. The Rayleigh range is estimated as 0.3 mm. The mirror is mounted on an xyz translation stage which facilitates micrometer control along three orthogonal axes. Specifically, the z-direction (laser beam propagation) incorporates a wide range of $\sim$10 mm ($\pm$20 μm accuracy) to allow optimum scanning of the laser focus along the interaction region perpendicular to the TOF axis. Following a 3 m flight path, ions are detected by a multi-channel plate detector (Galileo), maintained at a voltage of $-$2.1kV, before averaged data is collected over 5000 sweeps on a digital oscilloscope (Tektronix TDS7104). A PC installed with GRAMS/32 software [15] (Galactic) is used for mass/charge calibration of the TOF spectra and subsequent data analysis. In this manner, averaged TOF mass spectra are collected as a function of z for a fixed peak laser intensity I_o.

Femtosecond ionization was performed using the Ti:sapphire kilohertz laser system at the Lund Laser Center (LLC) which has been described in detail elsewhere [16, 17]. Briefly, low energy, (5 nJ, 35 fs, 76 MHz) ultrashort pulses from an oscillator are stretched in time in a grating based stretcher before being amplified at 1 kHz repetition rate, in a regenerative and two Ti: sapphire multipass amplifiers, pumped by two Nd:YLF lasers, reaching energies of 4–5 mJ. The amplified pulses are re-compressed using a grating compressor, yielding pulses as short as 35 fs and 2.5 mJ. Gain narrowing of the system is reduced by an acousto-optical programmable dispersive light modulator (Dazzler, Fastlite, Palaiseau, France). A pulse post compressor [18, 19] based on a gas filled hollow waveguide (normally Argon at $\sim$190 torr) followed by a dispersive line of chirped mirrors delivered pulses as short as 20 fs, with $\sim$0.5 mJ per pulse.

Results and Discussion

Intensity selective z-scanning measurements were carried out using the 0.4 mm diameter hole and the 0.8 mm wide slit as the extraction optic. In the following section the data recorded using the 0.4 mm aperture is discussed in detail while comparative results with the 0.8 mm slit are shown later. Figure 2 displays TOF mass spectra of benzene-d1 (C_6H_5D) at z-positions of +4.45, $\pm$1.8, and 0 mm. The position of the focal spot corre-

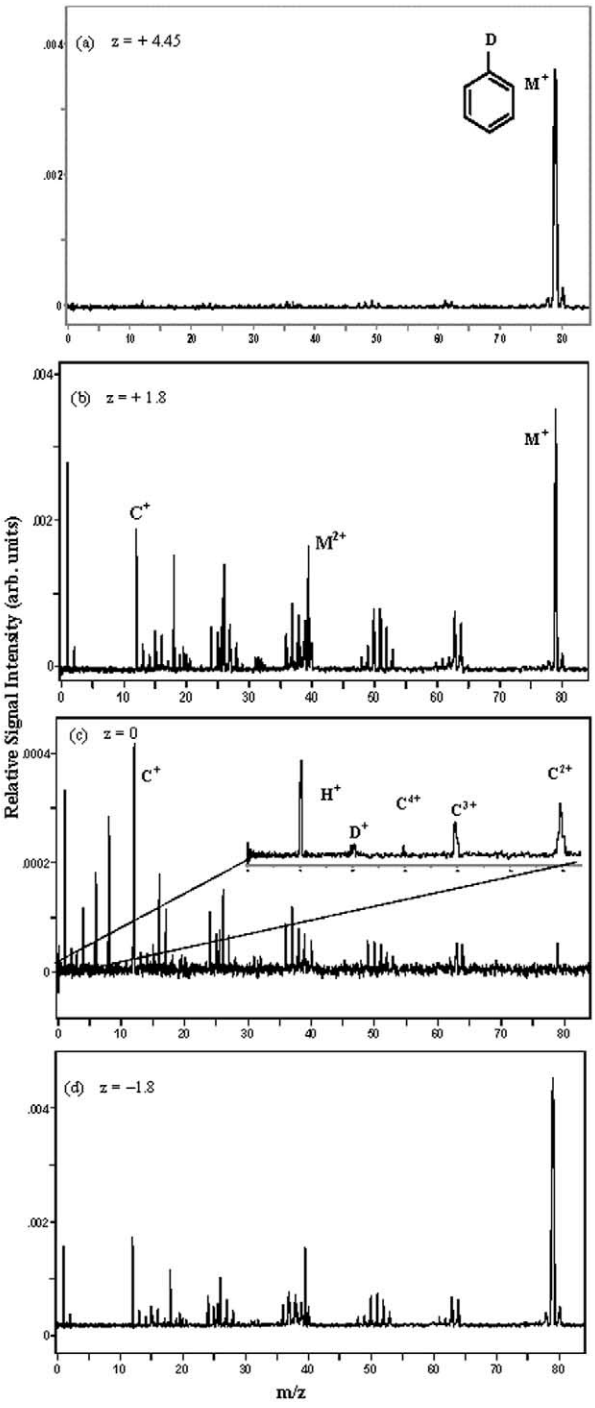

Figure 2. Mass spectra of deuterated benzene (C_6H_5D) as a function of z. For (**a**) z = +4.45 mm, only the molecular ion is detected. At z = $\pm$1.8 mm (**b**) and (**d**) low intensity regions dominate the morphology of the mass spectra obtained, and a strong molecular ion is detected. In contrast at z = 0, (**c**) only the highest intensity regions are accessed and multiply charged atomic ions are dominant.

sponding to z = 0, is defined as the optimum alignment of the focal spot in relation to the ion extraction optic. In other words the center of the focal spot where $I = I_o$ lies centrally on the TOF axis. The z = 0 position was calibrated by initial geometrical alignment of the focal spot with respect to the TOF axis and subsequent precision alignment (±20 μm) optimised on the ion yield of the highest charged atomic state (Kr^{6+}), which is produced at the highest laser intensity at the center of the laser focus.

The spectrum corresponding to z = +4.45 mm exhibits almost exclusive benzene-d1 cation which is characteristic of femtosecond excitation of benzene and its deuterated derivatives at the lower peak intensity regime (10^{13}–10^{14} Wcm^{-2}) [20, 21]. For z = ±1.8 mm, the spectra exhibits strong cation (M^+, *m/z* = 79) and dication (M^{2+}, *m/z* = 79/2) in addition to an increased signal from fragmentation and singly charged C^+ and H^+ ions. As the beam waist is scanned across the probed part of the interaction region, the peak intensity exposed to the detector first increases. This is reflected in the spectra recorded for z = 0 mm, which exhibits a reduced ion yield for the benzene-d1 cation and dication. In contrast, the multiply charged carbon ions, C^{z+} (z = 2–4) dominate the spectra at the z = 0 position. At z = 0, the ion yield is reduced by an order of magnitude, indicating that the intensities pertaining to the volume slices selected by the aperture are considerably affecting the ion yield, a phenomenon described recently by McKenna et al. [22] for single photon ionization. As the minimum beam waist is moved beyond the TOF axis (defined as negative z direction) the cation (and dication) yield increases while the relative yield of the multiply charged carbon ions is reduced. In fact, it can be seen that the spectra corresponding to z = ±1.8 are almost identical, (in relative fragmentation terms) corresponding to each "wing" of the laser focus. It should be noted that preliminary investigations of the z-dependence of the laser focus in relation to the extraction aperture were reported recently by this group [23] and revealed an almost identical pattern for the molecule 1-nitro-pyrene to that mentioned above for benzene. The effect of varying z-position on singly and multiply charged fragments is discussed further by looking at the ion yield (obtained by integrating the specific peaks) of the aforementioned fragments over the entire z-range attainable.

Figure 3 displays the relative ion yield of specific ion peaks from benzene as a function of (Figure 3a) z-position of the focal spot and (Figure 3b) the corresponding on-axis intensity calculated using eq 1 for r = 0, and the Rayleigh range (z_0) = 0.3 mm. The ion plots are of the benzene cation M^+, the dication M^{2+}, and the singly and multiply charged carbon ions C^{z+} (z = 1–4). It can clearly be seen that the fragments exhibit a similar, but not identical, distribution as a function of position of the laser focus with respect to the TOF axis and is a direct consequence of the spatial variation of the laser intensity around the focus. The benzene-d1 cation exhibits a symmetric distribution

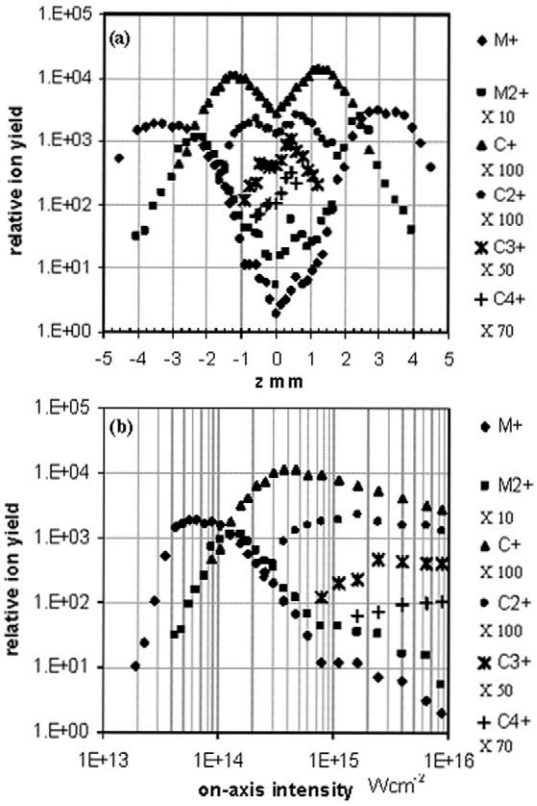

Figure 3. Relative ion yield of singly and multiply charged species of benzene-d1 as a function of (**a**) z position of the focal spot in relation to the extraction slit (0.4 mm wide). (**b**) corresponding on-axis peak intensity. In each case points are subject to ±20 μm. Multiplication factors have been added as indicated and are used only for ease of viewing.

for each "wing" of the laser pulse where the ion yield is at a maximum. This can be explained in qualitative terms by considering the volumetric intensity distribution of the laser focus. The scanning range in z of the focus is ~9 mm and the diameter of the pin hole on the second optic is 0.4 mm. When the beam is displaced ~3 mm in the z direction, (equivalent to ~10 Rayleigh ranges) from the central focal spot, the detector is exposed to a region of the laser focus where the volume (V_1 say) containing the intensity corresponding to prominent cation production is much larger than it is when the central focal region is exposed at z = 0. It is clear from Figure 3a that the z = 3 mm corresponds to maximum cation production. This position relates to an on-axis intensity of ~8×10^{13} Wcm^{-2} from Figure 3b. In contrast to this, a minimum is observed for the benzene cation yield where the central part of the focal beam (beam waist) is directly exposed to the extraction aperture at z = 0. In this instance, the volume that is exposed to the extraction slit which corresponds to cation production is less than V_1 mentioned above. The volumes exposed to the detector for a particular z position can be estimated to a first approximation by assuming a cone shaped interaction volume determined by the expanding waist (*w*) of the laser focus and the width of the extraction aperture. It can, therefore, be

determined that the ratio of volume slices exposed to the detector for z = 3 and z = 0 mm is of the order of 45 while the ratio of ion yield of the cation at the corresponding positions is significantly higher $\sim 1.5 \times 10^3$, as can be seen in Figure 3a. Therefore, the reduction in the observed ion yield at z = 0 is not simply a consequence of a reduction in the volume exposed to the detector but a greater contribution from a confocal volume(s) corresponding to higher intensity processes as represented by the isointensity contours depicted in Figure 1.

The benzene-d1 dication follows a similar distribution to that of the cation where maxima are observed for each wing of the laser focus (z ~ ±2 mm) and a minima for z = 0. In fact all of the singly charged $CmHn^+$ fragments (not shown) display this characteristic symmetric distribution. However, the z-range over which the ions are detected differs, with the benzene cation exhibiting the largest attainable range. The spatial weightings described below can be used to explain this.

In the case of atoms, where ionization is the only channel, this can be explained by a simplified discussion. For studies carried out on Xenon [6, 7] in the intensity averaged mode, (where the extraction aperture is several times the Rayleigh range), Xe^+ ions contribute the greatest yield to the mass spectrum since singly charged ions are generated within a much larger volume than any of the other higher charge states. For absolute peak intensities of I_0 that are greater than the saturation intensity required to create Xe^+, the spatial weighting factor grows as $I_0^{3/2}$ [24]. The higher charge states are only produced near the center of the focus since they require higher intensities. An enhancement of single ions is observed as a consequence of the volumetric weightings. Furthermore, when a small slit is in place that exposes only the Rayleigh range to the detector, then because of the spatial selectivity, the various charge states of Xe will have different volumetric weightings than when the entire focus is exposed to the detector.

As stated previously, intensity selective z-scanning measurements were also carried out using a larger extraction aperture, namely a 0.8 mm slit and at different sample operational pressures. Figure 4 shows the normalized ion yield as a function of z (and on-axis intensity) for the benzene-d1 molecular ion at gas pressures of 5.2×10^{-7} torr with the 0.4 mm aperture and 7.2 and 2.0×10^{-7} torr with the 0.8 mm slit. At all pressures using both extraction apertures, the ion yield exhibits the same characteristic distribution as a function of z. However, it can be seen that in the case of the 0.8 mm slit, the $C_6H_5D^+$ ion yield has fallen by a factor of ~10 at the z = 0 position for a gas pressure of 7.2×10^{-7} torr and by a factor of ~100 for the lower pressure of 2.0×10^{-7} torr. Therefore, in this case the size of the ion yield at the observed minima is directly related to the number density of the target. However, with the 0.4 mm aperture at a pressure approximately midway between the two stated above, the ion yield drops by a factor of ~1000 at the z = 0 position. It can be seen that

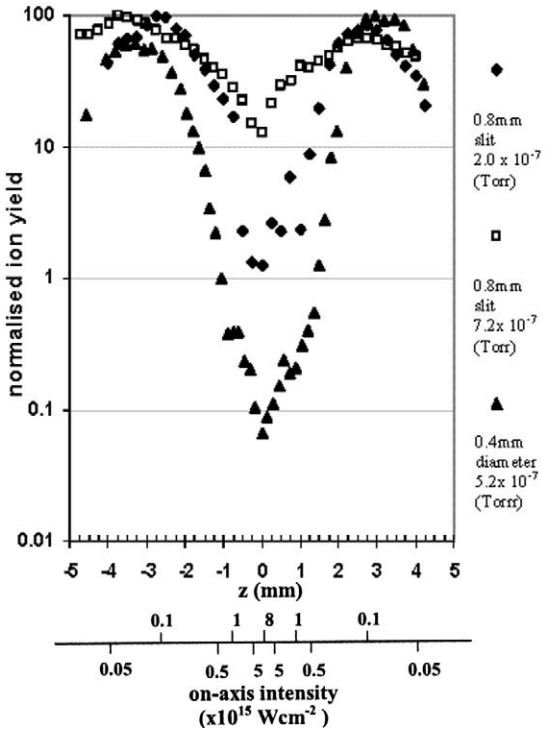

Figure 4. Ion distribution of benzene-d1 molecular ion as a function of pressure and extraction optic size.

the volumetric weightings of the isointensity contours accessed are ultimately dictating the ion plots observed, highlighting the significance of the isointensity volumes accessed by an extraction aperture that is comparable with or less than the Rayleigh range and also the increased spatial resolution obtained.

Applying the same principles described for atoms [7] to molecules is inherently more complicated due to the competing processes of ionization and dissociation, with the latter dominating at higher intensities. Additionally, coulomb explosion [25] of highly charged transient species giving rise to multiply charged atomic ions C^{z+} (z = 1–4) occurs at higher intensities. The distribution of the carbon ions C^{z+} (z = 1–4) as a function of z position are also depicted in Figure 3a. Maximum ion yields are detected at ±z positions where the volume exposed to the detector corresponding to intensities high enough to permit coulomb explosion is at a maximum. In the case of the C^{z+} (z = 1–4) ions, Figure 3b shows that as the focus is moved towards the z = 0 position and higher intensity volumes are accessed, higher charge states of the C^{z+} ion are detected. The minimum on axis appearance intensities the C^+, C^{2+}, C^{3+}, and C^{4+} are detected are 9×10^{13}, 3×10^{14}, 8×10^{14}, and 1.8×10^{15} Wcm^{-2} respectively. It cannot be unambiguously stated that the above intensities are "onset" intensities for coulomb explosion since the extraction aperture will still accept ions over a limited range of intensities. Table 1 shows the range of on-axis intensities accessed by the 0.4 mm aperture that correspond to appearance intensities for the C^{z+} fragments.

Table 1. Experimental range of appearance intensities for singly and multiply charged carbon ions

Coulomb explosion fragment	C^+	C^{2+}	C^{3+}	C^{4+}
Range of appearance intensities ($\times 10^{15}$ Wcm^{-2})	0.08–0.12	0.25–0.44	0.79–2.14	1.60–5.90

These values agree well with the work of Hankin et al. for coulomb explosion onset at 2×10^{14} Wcm^{-2} using tunneling theory [2]. In addition, at a relatively low intensity of 9×10^{13} Wcm^{-2}, the C^+ ion yield is not attributable to a coulomb explosion mechanism but to dissociation from the molecular ion [20].

Figure 5 displays the ion yield of the multiply charged atomic ions C^{z+} (z = 1–4) as a function of z for benzene-d1 using (Figure 5a) the 0.4 mm pin hole and (Figure 5b) 0.8 mm slit extraction regions. For the 0.8 mm slit, the singly charged C^+ ion displays a similar characteristic distribution as with the 0.4 mm aperture. The distribution of the remaining carbon ions C^{z+} (z = 2–4) when the 0.8 mm slit is inserted, Figure 5b, is significantly different from that when the 0.4 mm aperture is used. In the former case, for each of the carbon ions (C^{z+} z = 2–4) a continuous curve is observed with a maxima corresponding to z = 0. It can be shown using ion simulation software SIMION [26] that the extraction aperture accepts ions from an interaction region that is at least the width of the slit itself.

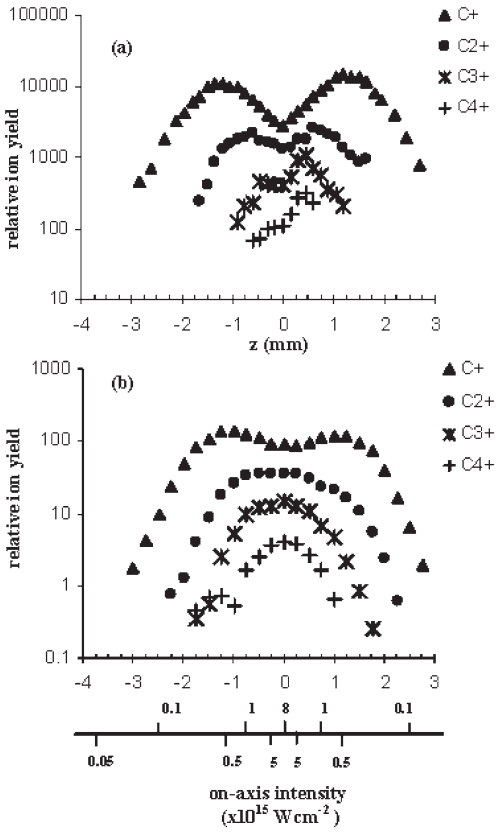

Figure 5. Ion yield of the multiply charged atomic ions C^{z+} (z = 1–4) as a function of z (and on-axis intensity) for benzene-d1 using (**a**) the 0.4 mm pin hole at a pressure of 5.2×10^{-7} torr and (**b**) the 0.8 mm slit at a pressure of 7.2×10^{-7} torr.

Thus, as a result of the larger extraction aperture (more than twice the Rayleigh range), when the central region of the focus is exposed to the detector, a relatively wide range of peak intensities is accessed. Specifically, over 0.4 mm (half the width of the extraction slit), at the z = 0 position, on-axis intensities can be calculated as $3–8.0 \times 10^{15}$ Wcm^{-2} for each "wing" of the focus (compare this with $6–8 \times 10^{15}$ Wcm^{-2} for the aperture). Therefore, the intensity selection "slice" is not small enough to access specific intensity contours relating to intensity selective volumes corresponding to dominant coulomb explosion of C^{z+} (z = 2–4), which occurs within the smaller, higher intensity volumes. In other words, even with a 0.8 mm slit ($\sim 2.6 \times z_R$) we still have a scenario where the larger confocal volumes of lower intensity ($<I_0$), significantly determine the resultant ionization/coulomb explosions processes.

Conclusions

The present study employs a tiny extraction aperture (0.4 mm) within a time of flight mass spectrometer to investigate the ionization/dissociation of benzene-d1 in intense laser fields. However, the technique adopted differs from conventional studies in that it concentrates on the ion distribution of various fragments as a function of position of the focus spot in relation to the extraction region for a constant peak intensity I_0. By scanning the focal spot along the direction of propagation of the laser beam (z), selective intensity regions were accessed by the detector. The resultant TOF mass spectra varied significantly, reflecting the range of intensities and the volumetric weightings accessed by scanning the focus spot.

Ion distributions for the benzene cation, dication, and multiply charged carbon ions (C^{z+} z = 1–4) were plotted as a function of z-position. All fragments exhibited an approximate symmetric distribution for each "wing" of the laser pulse where the ion yield is at a maximum. The observed patterns are a direct consequence of the spatial variation of the laser intensity around the focus. Low intensity regions of the focus spot occupy a much larger geometrical volume than the peak intensity, as depicted by the "peanut-shaped" isointensity contours. Thus, when the focus was displaced ~3 mm from I_0, large, low intensity regions ($\sim 8 \times 10^{13}$ Wcm^{-2}) are accessed and the cation dominated the resultant mass spectra. In contrast, at the z = 0 position, the isointensity contours of high intensity regions are spatially selected and multiply charged carbon ions, synonymous with coulomb explosions of highly charged transient species, dominated the mass spectra. In addition, almost no cation was observed.

Many traditional intensity dependent investigations

have relied on inserting additional optics into the beam path (neutral density filters) to control the peak intensity I_0. This may distort the overall beam quality and will inevitably lengthen the pulse duration somewhat. By sampling only a small fraction of the laser focus (<Rayleigh range) and scanning across the laser focus relative to the TOF axis, precise intensities can be selected without altering the beam profile. In addition, the formation of individual ions (singly and multiply charged) may ultimately be associated with precise geometrical interaction volumes within the laser focus and therefore accurate intensity dependent measurements can be made. A similar technique has been described by Witzel et al. outlining the applications of a spatially confining TOF mass spectrometer [27].

The above study has focused on the gas phase sample of benzene. It should be noted that the Glasgow group has carried out similar studies [23] on the solid-phase nitro-aromatic molecule 1-nitropyrene ($C_{16}H_9NO_2$). Analogous results have been obtained underlining the potential universality of the z-scan technique. In addition, the focus position of the beam was varied in the y direction (perpendicular to TOF axis and z) in relation to the extraction aperture. Preliminary results reveal that the y dependence is as critical as, if not more than, the z-dependence of the focus on the resultant mass spectra. Further studies are required utilizing a smaller acceptance aperture $\ll$ Rayleigh range, to elucidate ionization processes such as multiphoton and field ionization and the formation of multiply charged molecular and atomic ions within a high intensity laser-molecule interaction zone. With an increased spatial resolution, the resultant ion distributions may reveal important features that are masked when a range of intensities is accessed by the detector, and the larger confocal volumes dominate [9].

It is important to note, however, that in terms of analytical purposes, detection of the molecular ion is essential and for some time femtosecond lasers coupled with TOF mass spectrometry (FLMS) have facilitated these studies [28–30], generally using an extraction aperture considerably larger than the Rayleigh range. In this scenario, the lower intensity, large confocal volumes dominate, and strong molecular parents and structure specific fragments are detected. Therefore, it may be useful to adopt a similar technique to that outlined in the present study, utilizing a tiny pin hole for extraction of ions but at a considerably lower intensity ($\sim 10^{13}$ Wcm^{-2}). Thus, at lower focused intensities a "soft" femtosecond ionization regime dominates, however, the size and energy of the laser systems could be considerably smaller for femtosecond analytical studies of molecules.

Finally, many discrepancies have arisen in the data of different authors when investigating the same analyte under almost identical laser conditions [10, 31]. The position of the focus spot in relation to the acceptance volume, as well as the dimensions of the acceptance volume itself have been identified as crucial experimental parameters for a more meaningful comparison of such data. It has been shown in the present work that the ion yield of specific singly and multiply charged ions varies significantly depending on these parameters.

Acknowledgments

This work was funded by the European Community under the program Improving Human Potential—Access to Research Infrastructures, contract no. HPRI-CT-1999-00041. PMcK is supported by a Royal Society of Edinburgh/SEELLD research fellowship. JMY acknowledges support from the China Scholarship Council and SS acknowledges support from the Japan Society for the Promotion of Science.

References

1. Banerjee, S.; Ravindra Kumar, G.; Matusek, D, R. Intensity-selective, field-induced dissociative ionization of CS2 by fs duration light pulses. *J. Phys. B* **1999,** *32*, 4277–4292.
2. Hankin, S. M.; Villeneuve, D. M.; Corkum, P. B.; Rayner, D. M.; Intense field ionization rates in atoms and molecules. *Phys. Rev. A* **2001,** *64*, 013405-1–013405-12.
3. Posthumus, J. *Molecules and Clusters in Intense Laser Fields*; Cambridge University Press: Cambridge, MA, 2001; pp 27–83.
4. Talebpour, A.; Chin, C. Y.; Chin, S. L.; Population trapping in rare gases. *J. Phys. B* **1996,** *29*, 5725–5733.
5. Jones, R. R. Interference effects in the multiphoton ionization of sodium. *Phys. Rev. Lett.* **1995,** *74*, 1091–1094.
6. Hansch, P.; Walker, M. A.; Van Woerkom, L. D. Spatially dependent multiphoton multiple ionization. *Phys. Rev. A* **1996,** *54*, R2559–R2562.
7. El-Zein, A. A. A.; McKenna, P.; Bryan, W. A.; Johnston, I. M. G.; Goodworth, T. R. J.; Sanderson, J. H.; Williams, I. D.; Newell, W. R.; Taday, P. F.; Divall, E.; Langley, A. J. A detailed study of multiply charged ion production within a high intensity laser focus. *Physica Scripta* **2001,** *T92*, 119–121.
8. Augst, S.; Meyerhofer, D. D.; Strickland, D.; Chin, S. L.; Laser ionization of noble gases by coulomb-barrier suppression. *J. Opt. Soc. Am. B* **1991,** *8*, 858.
9. Greenwood, J. B.; Johnston, I. M. G.; McKenna, P.; Williams, I. D.; Goodworth, T. R. J.; Sanderson, J. H.; Bryan, W. A.; El-Zein, A. A. A.; Newell, W. R.; Langley, A. J.; Divall, E. Suppression of multiple ionization of atomic ions in intense ultra fast laser pulses. *Phys. Rev. Lett.* **2002,** *88*, 233001/1–233001/4.
10. Robson, L.; Ledingham, K. W. D.; Tasker, A. D.; McKenna, P.; McCanny, T.; Kosmidis, C.; Jaroszynski, D. A.; Jones, D. R.; Issac, R. C.; Jamieson, S. Ionization and fragmentation of polycyclic aromatic hydrocarbons by femtosecond laser pulses at wavelengths resonant with cation transitions. *Chem. Phys. Lett.* **2002,** *360*, 382–389.
11. Tasker, A. D.; Robson, L.; Ledingham, K. W. D.; McCanny, T.; Hankin, S. M.; McKenna, P.; Kosmidis, C.; Jaroszynski, D. A.; Jones, D. R. A high mass resolution study of the interaction of aromatic and nitro-aromatic molecules with intense laser fields. *J. Phys. Chem.* **2002,** *106*, 4005.
12. Auguste, T.; Monot, P.; Lompre, L. A.; Mainfray, G.; Manus, C. Multiply charged ions produced in noble gases by a 1 ps laser pulse at l = 1053 nm. *J. Phys. B* **1992,** *25*, 4181–4194.
13. Wiley, W. C.; McLaren, I. H. Time-of-flight mass spectrometer with improved resolution. *Rev. Sci. Inst.* **1955,** *26*, 1150.
14. Mamyrin, B. A.; Karataev, V. I., Shmikk, D. V., Zagulin, V. A. The mass-reflectron, a new nonmagnetic time-of-flight mass spectrometer with high resolution. *Sov. Phys. JETP.* **1973,** *37*, 45.

15. Galactic Ind. Corp.; Grams/32. 1999. http://www.galactic.com.
16. Mauritsson, J. Ph.D Thesis, Lund Institute of Technology, Lund Reports on Atomic Physics LRAP, 2003; p 312.
17. Lopez-Martens, R.; Mauritsson, J.; Johansson, J.; Norin, J.; L'Huillier, A. Time-frequency characterization of high-order harmonic pulses. *Eur. Phys. J. D* **2003,** *26*, 105–109.
18. Nisoli, M.; De Silvestri, S.; Svelto, O.; Szipocs, R.; Ferencz, K.; Spielman, C.; Sartania, S.; Krausz, F. Compression of high-energy laser pulses below 5 fs. *Opt. Lett.* **1997,** *22*, 522–524.
19. Sartania, S.; Cheng, Z.; Lenzner, M.; Tempea, G.; Spielmann, C.; Krausz, F.; Ferencz, K. Generation of O.1-TW 5-fs optical pulses at a 1-kHz repetition rate. *Opt. Lett.* **2002,** *22*, 1562–1564.
20. Castillejo, M.; Couris, S.; Koudoumas, E.; Martin, M. Ionization and fragmentation of aromatic and single-bonded hydrocarbons with 50 fs laser pulses at 800 nm. *Chem. Phys. Lett.* **1999,** *308*, 373–380.
21. Smith, D. J.; Ledingham, K. W. D.; Singhal, R. P.; Kilic, H. S.; McCanny, T.; Langley, A. J.; Taday, P. F.; Kosmidis, C. Time-of-flight mass spectrometry of aromatic molecules subjected to high intensity laser beams. *Rapid Commun. Mass Spectrom.* **1998,** *12*, 813.
22. McKenna, C.; van der Hart, H. W. Single- and two-photon ionization of neutral Ca. *J. Phys. B* **2003,** *36*, 1627–1643.
23. Tasker, A. D.; Robson, L.; Ledingham, K. W. D.; McCanny, T.; McKenna, P.; Kosmidis, C.; Jaroszynski, D. A. Femtosecond ionization and dissociation of laser desorbed nitro-PAHs. *Int. J. Mass Spectrom.* **2003,** *225*, 53–70.
24. L'Huillier, A.; Lompre, L. A.; Mainfray, G.; Manus, C. Multiply charged ions Induced by multiphoton absorption in rare gases at 0.53 mm. *Phys. Rev. A* **1983,** *27*, 2503–2512.
25. Tzallas, P.; Kosmidis, C.; Graham, P.; Ledingham, K. W. D.; McCanny, T.; Hankin, S. M.; Singhal, R. P.; Taday, P. F.; Langley, A. J. Coulomb explosion in aromatic molecules and their deuterated derivatives. *Chem. Phys. Lett.* **2000,** *332*, 236–242.
26. David Dahl. www.simion.com/; 2004.
27. Witzel, B.; Schröder, H.; Kaesdorf, S.; Kompa, K-L. Exact determination of spatially resolved ion concentration in focused laser beams. *Int. J. Mass Spectrom.* **1998,** *172*, 229–238.
28. Ledingham, K. W. D.; Singhal, R. P. High intensity laser mass spectrometry—A review. *Int. J. Mass Spectrom.* **1997, 163**, 149–168.
29. Hankin, S. M.; Tasker, A. D.; Robson, L.; Ledingham, K. W. D.; Fang, X.; McKenna, P.; Singhal, R. P.; Kosmidis, C.; Tzallas, P.; Jaroszynski, D. A.; Jones, D. R.; Issac, R. C.; Jamieson, S. Femtosecond laser time-of-flight mass spectrometry of labile molecular analytes: Laser-desorbed nitro-aromatic molecules. *Rapid Commun. Mass Spectrom.* **2002,** *16*, 111.
30. Weinkauf, R.; Aicher, P.; Wesley, G.; Grotemeyer, J.; Schlag, E. W.; Femtosecond versus nanosecond multiphoton ionization and dissociation of large molecules. *J. Phys. Chem.* **1994, 98**, 8381–8391.
31. Muller, A. M.; Uiterwaal, C. J. G. J.; Witzel, B.; Wanner, J.; Kompa, K-L. Photoionization and photofragmentation of gaseous toluene using 80 fs, 800 nm laser pulses. *J. Chem. Phys.* **2000,** *112*, 9289–9300.